ELSEVIER

Journal of Organometallic Chemistry 575 (1999) 200–208

Journal of Organometallic Chemistry

Syntheses, reactivity studies and structural characterisation of triruthenium carbonyl methoxynitrido clusters containing phosphine ligands

Kenneth Ka-Hong Lee, Wing-Tak Wong *

Department of Chemistry, The University of Hong Kong, Pokfulam Road, Hong Kong, Hong Kong

Received 21 July 1998

Abstract

The substitution reaction of the methoxynitrido cluster, $[Ru_3(CO)_9(\mu_3\text{-}CO)(\mu_3\text{-}NOMe)]$ **1** with PPh_3 affords both mono- and di-substituted products with the formulae $[Ru_3(CO)_8(\mu_3\text{-}CO)(\mu_3\text{-}NOMe)(PPh_3)]$ **2** and $[Ru_3(CO)_7(\mu_3\text{-}CO)(\mu_3\text{-}NOMe)(PPh_3)_2]$ **3**, respectively. When a bidentate phosphine such as bis(diphenylphosphino)methane (dppm) is used, $[Ru_3(CO)_7(\mu_3\text{-}CO)(\mu_3\text{-}NOMe)(\mu\text{-}dppm)]$ **4** is formed, in which the dppm ligand replaced two equatorial carbonyls from two adjacent Ru centres. Both clusters **3** and **4** are stable when heated, while vacuum pyrolysis of **2** yields a di-isocyanate cluster $[Ru_3(CO)_8(\mu\text{-}NCO)_2(PPh_3)_2]$ **5** with the two isocyanate ligands spanning over the open Ru···Ru edge on both sides of the Ru_3 plane.

Keywords: Ruthenium; Cluster; Methoxynitrido; Phosphine; Isocyanate

1. Introduction

In previous papers, the triruthenium methoxynitrido clusters, $[Ru_3(CO)_9(\mu_3\text{-}CO)(\mu_3\text{-}NOMe)]$ and $[Ru_3(\mu\text{-}H)_2(CO)_9(\mu_3\text{-}NOMe)]$ were reported to be synthetic precursors for nitrido and/or nitrene species [1–3] such as $[Ru_4(CO)_{12}(\mu_4\text{-}N)(\mu\text{-}OMe)]$, $[Ru_6(CO)_{13}(\mu\text{-}CO)(\mu_5\text{-}N)(\mu_3\text{-}NH)(\mu_3\text{-}OMe)\{\mu\text{-}\eta^2\text{-}C(O)OMe\}_2]$ and $[Ru_6(CO)_{16}(\mu\text{-}CO)_2(\mu_4\text{-}NH)(\mu\text{-}OMe)(\mu\text{-}R)]$ (where R = H, OMe and NCO). The isolation of the quadruply bridging nitrene (μ_4-NH) containing clusters is particularly interesting since this moiety has only been isolated successfully once from the protonation of the $[Ru_4(\mu_4\text{-}N)(CO)_{12}]^-$ anion, in the presence of diphenylacetylene as a structural stabiliser [4]. The polynuclear μ_4-NH species formed from the methoxynitrido clusters are believed to originate from the thermolytic N–O bond cleavage of the methoxynitrido moiety. However, no detailed reaction pathways leading to these compounds have been elucidated so far. Recently, the phosphine-substituted derivative of the closely related nitrene clusters $[Ru_3(CO)_9(\mu_3\text{-}CO)(\mu_3\text{-}NPh)]$ [5] was synthesised which, substantially assisted our investigation of the substitution reaction of the methoxynitrido cluster, $[Ru_3(CO)_9(\mu_3\text{-}CO)(\mu_3\text{-}NOMe)]$ in two directions. First of all, we extended our investigation into the chemistry of methoxynitrido clusters in the hope of developing the chemical reactivity of those newly synthesised substituted methoxynitrido clusters by varying both their electronic and structural features. Furthermore, we believe that introducing a phosphine ligand may give us some insight into the understanding of possible mechanisms for the formation of these nitrido and nitrene species. This is because the molecular symmetry of the phosphine containing derivatives are lower and the interpretation of spectroscopic data will be simpler. In addition the use of these clusters as starting materials for the preparation of μ_4-nitrene containing species allows the metal core rearrangement process to be determined.

* Corresponding author. Fax: +852-25472933; e-mail: wtwong@hkucc.hku.hk.

0022-328X/99/$ - see front matter
PII: S0022-328X(98)00994-2

Table 1
Spectroscopic data for clusters **2**–**5**

Cluster	IR (ν_{CO}), [a] cm^{-1}	^{1}H-NMR, δ [b]	^{31}P-NMR, δ [b]	MS, [c] m/z
2	2084s, 2057s, 2020vs, 2015sh, 1996s, 1958m, 1716s	7.45 [m, 15H, phenyl], 3.52 [s, 3H, methoxy]	42.20	862 (862)
3	2062s, 2022s, 2005vs, 1970s, 1943m, 1684m	7.46 [m, 30H, phenyl], 3.51 [s, 3H, methoxy]	42.74, 35.88	1096 (1096)
4	2068s, 2018vs, 2004s, 1988w, 1976m, 1960w, 1713m	7.43 [m, 10H, phenyl], 7.19 [m, 6H, phenyl], 7.03 [m, 4H, phenyl], 3.97 [q, J_{PH} 12.2Hz, 1H, –CH_2–], 3.43 [q, J_{PH} 11.4Hz, 1H, –CH_2–], 3.18 [s, 3H, methoxy]	25.44	956 (956)
5	2179vs, 2071s, 2019s, 2003m, 1953w	7.25 [m, 30H, phenyl]	21.27	1135 (1135)

[a] Recorded in CH_2Cl_2.
[b] Recorded in CD_2Cl_2.
[c] Calculated value in parentheses.

2. Results and discussion

2.1. Reaction of cluster *1* with triphenylphosphine

The reaction between stoichiometric amounts of both $[Ru_3(CO)_9(\mu_3\text{-}CO)(\mu_3\text{-}NOMe)]$ **1** and triphenylphosphine (PPh_3), in THF, at room temperature for 3 days afforded the isolation of two yellow compounds, $[Ru_3(CO)_8(\mu_3\text{-}CO)(\mu_3\text{-}NOMe)(PPh_3)]$ **2** and $[Ru_3(CO)_7(\mu_3\text{-}CO)(\mu_3\text{-}NOMe)(PPh_3)_2]$ **3** in 29 and 7% yields, respectively. Both **2** and **3** were characterised fully by spectroscopic methods and the related data are summarised in Table 1.

The IR spectra of **2** and **3** resembled closely the mono- and di-substituted phenylimido derivatives $[Ru_3(CO)_{9-n}(\mu_3\text{-}CO)(\mu_3\text{-}NPh)(PPh_3)_n]$ (where $n = 1$ or 2) which have been reported previously by Bott and Richmond from the reaction of $[Ru_3(CO)_9(\mu_3\text{-}CO)(\mu_3\text{-}NPh)]$ with triphenylphosphine [5]. The formulations of **2** and **3** were established first by positive mass spectra which are consistent with triruthenium species on the basis of the patterns of peak envelopes. The ^{1}H-NMR spectra of **2** and **3** are similar in that they both show proton resonances attributable to the phenyl rings and methoxy group only, but the relative intensities are in ratios of 5:1 and 10:1, respectively. However, the ^{31}P-NMR spectra provided additional information about the orientation of the PPh_3 ligands in the co-ordinated compounds. In contrast to a singlet at 42.20 ppm for cluster **2**, the spectrum of **3** revealed the presence of two singlet peaks with almost equal intensity at 42.74 and 35.88 ppm which were assigned to both axial and equatorial co-ordinated phosphine ligands. In addition to the signals due to the terminal CO, the IR of both **2** and **3** showed their characteristic ν_{CO} for the triply bridging carbonyl groups at 1716 and 1684 cm^{-1}, respectively.

Crystals of both **2** and **3** with qualities suitable for X-ray analysis were obtained by slow evaporation of their respective saturated solution mixtures of *n*-hexane and dichloromethane at room temperature. The molecular structure of **2** and some selected bond parameters of **2** are depicted in Fig. 1 and Table 2, respectively. The molecule of **2** is closely related to the structure of **1** with one of the axial carbonyl groups replaced by a triphenylphosphine ligand. The triruthenium methoxynitrido metal framework is composed of an equilateral triruthenium plane with average Ru–Ru distance of 2.775(1) Å which is symmetrically capped on both sides by a triply-bridged methoxynitrido and μ_3-bridging carbonyl group. The average Ru–N bond length [2.024(6) Å] is comparable to that in **1** (average Ru–N 2.02(3) Å) [6] and $[Ru_3(CO)_9(\mu_3\text{-}CO)(\mu_3\text{-}NPh)]$ (2.054(4) Å) [7]. The N(1)–O(10) bond length is found to be 1.414(8) Å, and is slightly shorter than that in **1** (1.433(6) Å). The PPh_3 ligand is co-ordinated in an axial position with Ru(3)–P(1) distance of 2.377(2) Å.

The molecular structure of **3**, from X-ray structural analysis, is shown in Fig. 2 while the important structural parameters are given in Table 3. The molecule of **3**, as expected, consists of a central triruthenium methoxynitrido core similar to the structures of **1** and **2** except that there are two co-ordinated phosphine ligands attached by two separate metal centres. The solution spectroscopic data including the ^{31}P-NMR spectroscopic properties is consistent with the solid state structure. The solution spectrum of **3** revealed the presence of two different resonances for the phosphorus nuclei at 42.74 and 35.88 ppm for the PPh_3 moieties in the axial and equatorial position respectively. The metal-metal bonds within the ruthenium triangle span a narrow range from 2.758(2) to 2.798(2) Å while the nitrogen atom of the methoxynitrido ligand is capped slightly asymmetrically (Ru(1)–N(1) 2.02; Ru(2)–N(1) 2.01(1) and Ru(3)–N(1) 2.036(1) Å) over the triruthenium core so that the methoxynitrido moiety is displaced away from the metal centre with co-ordinated PPh_3 in an equatorial position. The two Ru–P bonds are almost equi-distant at (average 2.382(1) Å) but are slightly longer than that in **2** (2.377(2) Å).

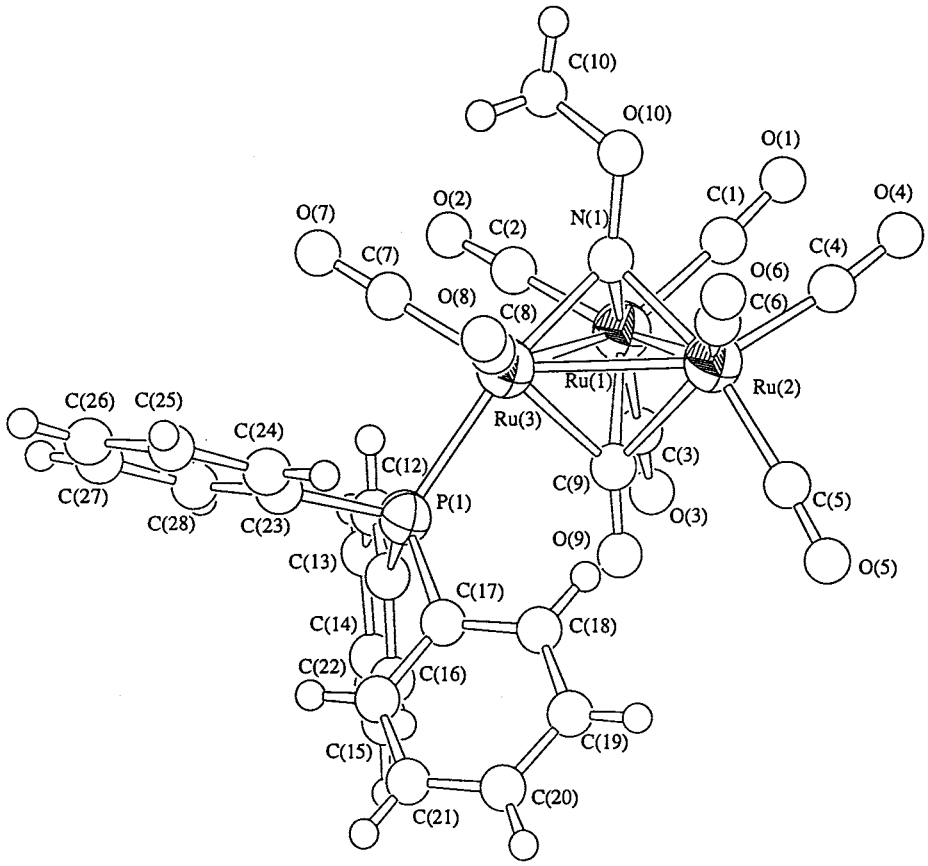

Fig. 1. The molecular structure of $[Ru_3(CO)_8(\mu_3\text{-}CO)(\mu_3\text{-}NOMe)(PPh_3)]$ **2** with the atom numbering scheme.

2.2. Reaction of cluster *1* with bidentate phosphine ligand

As cluster **1** is shown to readily undergo substitution of carbonyl groups by mono-dentate phosphine ligands to give phosphine-substituted methoxynitrido clusters which exhibit greater stability when compared with the parent compound. As a continuation, the synthesis of $[Ru_3(CO)_7(\mu_3\text{-}CO)(\mu_3\text{-}NOMe)(\mu\text{-}dppm)]$ was desired since previous studies of clusters bearing bidentate ligands have shown that they usually give extra stability and may be favourable for catalysis. For example, $[Ru_3(CO)_{10}(\mu\text{-}dppm)]$ had proved to be an active catalyst in the reductive carbonylation of nitrobenzene [8] in a solvent mixture of toluene + methanol at 170°C and 60 atm. of CO which afforded the corresponding carbamate, PhN(H)C(O)OMe.

Table 2
Selected bond lengths (Å) and angles (°) of cluster **2** with estimated S.D. in parentheses

Bond lengths (Å)			
Ru(1)–Ru(2)	2.765(1)	Ru(2)–Ru(3)	2.777(1)
Ru(1)–Ru(3)	2.784(1)	Ru(1)–N(1)	2.028(6)
Ru(2)–N(1)	2.014(6)	Ru(3)–N(1)	2.030(6)
Ru(3)–P(1)	2.377(2)	N(1)–O(10)	1.414(8)
O(10)–C(10)	1.41(1)		
Bond angles (°)			
Ru(1)–Ru(2)–Ru(3)	60.31(3)	Ru(2)–Ru(1)–Ru(3)	60.06(2)
Ru(1)–Ru(3)–Ru(2)	59.64(3)	Ru(1)–N(1)–Ru(2)	86.3(3)
Ru(2)–N(1)–Ru(3)	86.7(2)	Ru(1)–N(1)–Ru(3)	86.6(2)
Ru(2)–Ru(3)–P(1)	125.61(6)	N(1)–O(10)–C(10)	112.7(7)

Treatment of **1** with a stoichiometric quantity of bis(diphenylphosphino)methane, dppm in THF at room temperature for 3 d afforded other than the starting compound **1**, the isolation of two compounds, $[Ru_3(CO)_7(\mu_3\text{-}CO)(\mu_3\text{-}NOMe)(\mu\text{-}dppm)]$ **4** and $[Ru_3(CO)_{10}(\mu\text{-}dppm)]$ in 35 and 5% yields, respectively, as shown in Scheme 1. Cluster **4** can be obtained also in much higher yields with the aid of a stoichiometric amount of the decarbonylating reagent, Me_3NO in which the transient mono-co-ordinated $[Ru_3(CO)_8(\mu_3\text{-}CO)(\mu_3\text{-}NOMe)(dppm)]$ is formed after the reaction mixture has been stirred for several hours. Cluster **4** has been characterised fully and the spectroscopic data tabulated in Table 1. Similar to clusters **1**, **2** and **3**, the IR spectrum of **4** reveals a sharp μ_3-CO stretching at 1713cm^{-1}. In the ^{1}H-NMR spectrum, in addition to the resonance due to the methoxy group (3.18 ppm), signals responsible for the dppm were observed at δ 7.43–7.03 (phenyl) and 3.97–3.43 ($-CH_2-$). The ^{31}P-NMR spectrum suggested also the equivalent of two

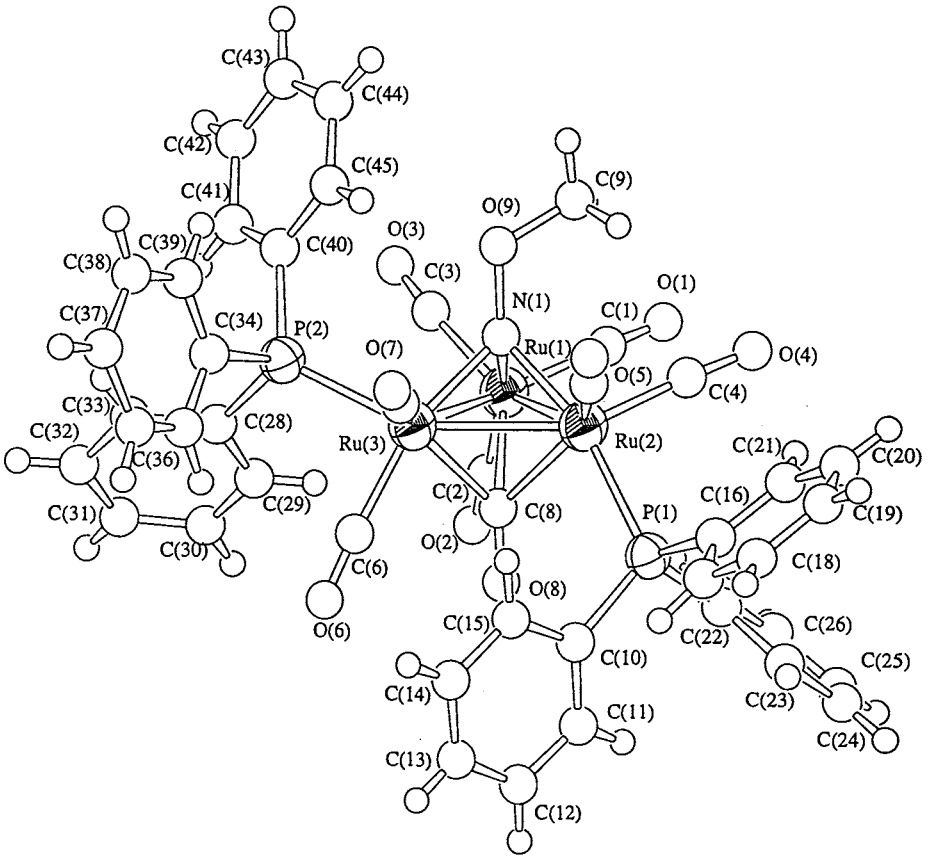

Fig. 2. The molecular structure of $[Ru_3(CO)_7(\mu_3\text{-}CO)(\mu_3\text{-}NOMe)(PPh_3)_2]$ **3** with the atom numbering scheme.

phosphorus atoms since only a singlet at 25.44 ppm was observed. The identity of the di-substitution of **4** by dppm was concluded by the positive mass spectrum which showed a parent ion peak centred at m/z 956 with a subsequent loss of eight carbonyl groups.

The molecular structure of **4** as determined by X-ray crystallography is depicted in Fig. 3 whereas some selected bond parameters are tabulated in Table 4. Single crystals of suitable size were grown by the diffusion of diethyl-ether into a saturated CH_2Cl_2 solution of **4** at room temperature. The solid-state structure of **4** is in good agreement with the spectroscopic data. The molecule of **4** consists essentially of a triruthenium methoxynitrido core (similar to **1**, **2** and **3**) with the bidentate dppm ligand, chelated on the Ru(2) and Ru(3) atoms, similar to the geometry of $[Ru_3(CO)_7(\mu_3\text{-}CO)(\mu_3\text{-}NPh)(\mu\text{-}dppm)]$ [8]. The three Ru–Ru bonds are essentially equi-distant (Ru(1)–Ru(2) 2.756(1), Ru(2)–Ru(3) 2.792(1) and Ru(1)–Ru(3) 2.747(1) Å) while the nitrogen atom is capped symmetrically over the metal core with an average Ru–N distance of 2.029(5) Å. The bidentate dppm ligand is spanned over the edge Ru(2)–Ru(3) whereas the two phosphorus atoms occupy the equatorial position with an average Ru–P separation of 2.338(3) Å which lies within a reasonable range to those values found in $[Ru_3(CO)_7(\mu_3\text{-}CO)(\mu_3\text{-}NPh)(\mu\text{-}dppm)]$ (2.344 Å) [8a] and $[Ru_3(CO)_7(\mu_3\text{-}NPh)_2(\mu\text{-}dppm)]$ (2.323 Å) [9]. Except for three CO bounded to Ru(1), both Ru(2) and Ru(3) are co-ordinated by two terminal carbonyls to give a precise cluster valence electron count of 48.

Table 3
Selected bond lengths (Å) and angles (°) of cluster **3** with estimated S.D. in parentheses

Bond lengths (Å)			
Ru(1)–Ru(2)	2.798(2)	Ru(2)–Ru(3)	2.758(2)
Ru(1)–Ru(3)	2.787(2)	Ru(1)–N(1)	2.02(1)
Ru(2)–N(1)	2.01(1)	Ru(3)–N(1)	2.036(10)
Ru(2)–P(1)	2.382(4)	Ru(3)–P(2)	2.381(4)
N(1)–O(9)	1.44(1)	O(9)–C(9)	1.44(2)
Bond angles (°)			
Ru(1)–Ru(2)–Ru(3)	60.22(4)	Ru(2)–Ru(1)–Ru(3)	59.19(4)
Ru(1)–Ru(3)–Ru(2)	60.60(4)	Ru(1)–N(1)–Ru(2)	88.1(4)
Ru(2)–N(1)–Ru(3)	86.0(4)	Ru(1)–N(1)–Ru(3)	86.9(4)
N(1)–O(9)–C(9)	113(1)		

2.3. Thermolytic reaction of clusters **2**–**4**

It was shown previously that thermolysis of cluster **1** results in the formation of high nuclearity clusters containing the quadruply bridging nitrene moiety [1,2].

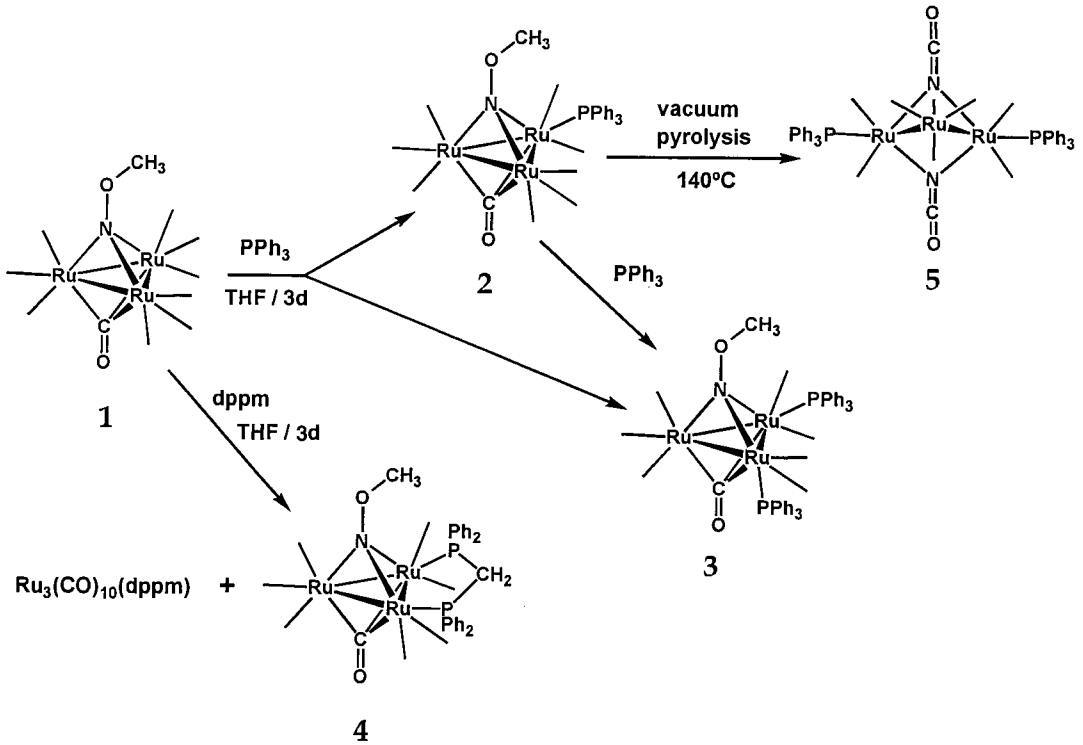

Scheme 1.

However, no unambiguous mechanism has been drawn so far. As a result, the phosphine-substituted derivatives of cluster **1** were chosen in order to study their thermolytic behaviour, in the hope of obtaining some μ_4-nitrene containing clusters which may give us some understanding of its formation.

As expected, those phosphine-derivatives, particularly clusters **3** and **4** are thermodynamically more stable than the parent cluster **1** since thermolysis of them in common high-boiling organic solvents such as toluene and *n*-octane does not give any observable change. In fact, the majority of the starting materials are stable when heated with very minor decomposition only. In comparison, cluster **2** seems to be more vulnerable and its thermolytic behaviour is focused upon especially.

Vacuum pyrolysis of cluster **2** in the solid state at 140°C afforded a number of yellow bands in which the relatively abundant one, $[Ru_3(CO)_8(\mu\text{-}NCO)_2(PPh_3)_2]$ **5**, was isolated (Scheme 1) and characterised by various spectroscopic methods (Table 1). The presence of co-ordinated PPh_3 ligands in **5** is revealed from both ^{1}H- and ^{31}P-NMR spectra of **5** in which the former shows a multiplet centred at δ 7.25 for the phenyl groups, while the latter signal indicates the chemical equivalent of two co-ordinated phosphine groups at 21.27 ppm. The IR spectrum of **5** shows the presence of a terminal carbonyl with a strong stretching frequency at 2179 cm^{-1} which is assigned to the ν(CO) of NCO. The mass spectrum of **5** exhibits a parent ion peak centred at m/z 1135 with an envelope distribution characteristic of three ruthenium atoms. In order to establish the molecular structure of **5,** crystals suitable for X-ray analysis were obtained by slow evaporation of a dichloromethane solution of **5** at -20°C.

The molecular structure of **5,** together with some important structural parameters, is depicted in Fig. 4 and Table 5, respectively. The crystal packing of **5** contains two CH_2Cl_2 molecules in the asymmetric unit as solvents of crystallisation. The molecule of **5** consists of an open triruthenium metal core with two isocyanate moieties bridged over the open Ru···Ru edge at both sides of the Ru_3 plane. The two Ru–Ru bonds are almost equi-distant (average 2.831(1) Å) while Ru(2)···Ru(3) is essentially non-bonding with a separation of 3.078(1) Å. The two isocyanate ligands are spanned symmetrically over the open edge with an average Ru–N distance of 2.183(9) and 2.178(1) Å and result in dihedral angles of 118.9 and 119.9° with respect to the triruthenium plane. Within the isocyanate groups, the mean N–C and C–O bonds are 1.155(1) and 1.205(1) Å, respectively which are in accordance with the reported values found in $[Ru_4(\mu\text{-}H)_3(\mu\text{-}NCO)(CO)_{12}]$ (N–C 1.153(7) and C–O 1.179(7) Å) [10]. The two isocyanate ligands are essentially linear with an average N–C–O bond angle of 177(1)°. Two additional PPh_3 ligands are co-ordinated to Ru(2) and Ru(3) in an equatorial position in contrast to **3**. The

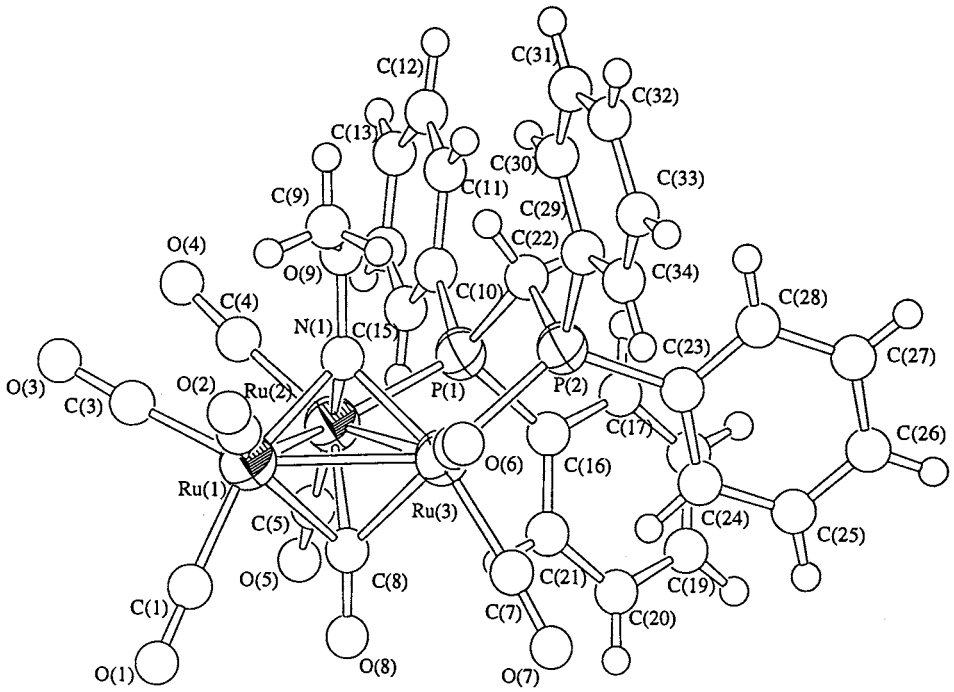

Fig. 3. The molecular structure of $[Ru_3(CO)_7(\mu_3\text{-}CO)(\mu_3\text{-}NOMe)(\mu\text{-}dppm)]$ **4** with the atom numbering scheme.

average Ru–P distance is also lengthened (2.408(1) Å) when compared to **2** (2.377(2) Å) and **3** (2.382(4) Å). Together with the two 3e-donating isocyanate ligands, the co-ordination sphere of **5** is filled with eight terminal CO and two PPh_3 ligands to give an electron count of 50, which is in accordance with the CVE count of triruthenium complex with two metal–metal bonds.

3. Conclusions

The incorporation of phosphine ligands to the triruthenium methoxynitrido cluster enhanced the thermal stability of the ruthenium compounds. The relative stabilities were reflected by the degree of substitution, i.e. di-substituted products such as clusters **3** and **4** are more thermally stable than cluster **2** since the latter may undergo thermolysis to give the isocyanate cluster **5**. The structural consequence for the generation of two μ-bridging isocyanate moieties in cluster **5** may be similar to that of our cluster example characterised previously, $[Ru_6(CO)_{16}(\mu\text{-}CO)_2(\mu_4\text{-}NH)(\mu\text{-}OMe)(\mu\text{-}NCO)]$, since both were formed in a condition of high CO pressure. Although cluster **5** was only isolated as one of the products in the reaction mixture, characterisation of the remaining products proceeded with difficulty since their respective yields were extremely low. From the colour of the products isolated from the reaction mixture, it is unlikely to have cluster-derivatives bearing the quadruply bridging nitrene (μ_4-NH) moieties formed from the pyrolysis of **2** since all of our μ_4-NH containing clusters characterised previously possess a distinctive blue colour.

Table 4
Selected bond lengths (Å) and angles (°) of cluster **4** with estimated S.D. in parentheses

Bond lengths (Å)			
Ru(1)–Ru(2)	2.756(1)	Ru(2)–Ru(3)	2.792(1)
Ru(1)–Ru(3)	2.747(1)	Ru(1)–N(1)	2.029(8)
Ru(2)–N(1)	2.032(8)	Ru(3)–N(1)	2.027(8)
Ru(2)–P(1)	2.314(3)	Ru(3)–P(2)	2.362(3)
N(1)–O(9)	1.431(10)	O(9)–C(9)	1.41(1)
P(1)–C(22)	1.83(1)	P(2)–C(22)	1.84(1)
Bond angles (°)			
Ru(1)–Ru(2)–Ru(3)	59.34(3)	Ru(2)–Ru(1)–Ru(3)	60.99(3)
Ru(1)–Ru(3)–Ru(2)	59.67(3)	Ru(1)–N(1)–Ru(2)	85.5(3)
Ru(2)–N(1)–Ru(3)	86.9(3)	Ru(1)–N(1)–Ru(3)	85.2(3)
Ru(2)–P(1)–C(22)	111.0(3)	Ru(3)–P(2)–C(22)	110.0(3)
N(1)–O(9)–C(9)	111.3(7)		

4. Experimental

4.1. General procedures

All manipulations were carried out under an inert atmosphere of argon with standard Schlenk technique, unless stated otherwise. Chemicals were used as received without further purification, unless stated otherwise. Trimethylamine-*N*-oxide was dried by azeotropic distillation and sublimed prior to use. Solvents were dried according to standard methods. Preparative thin-

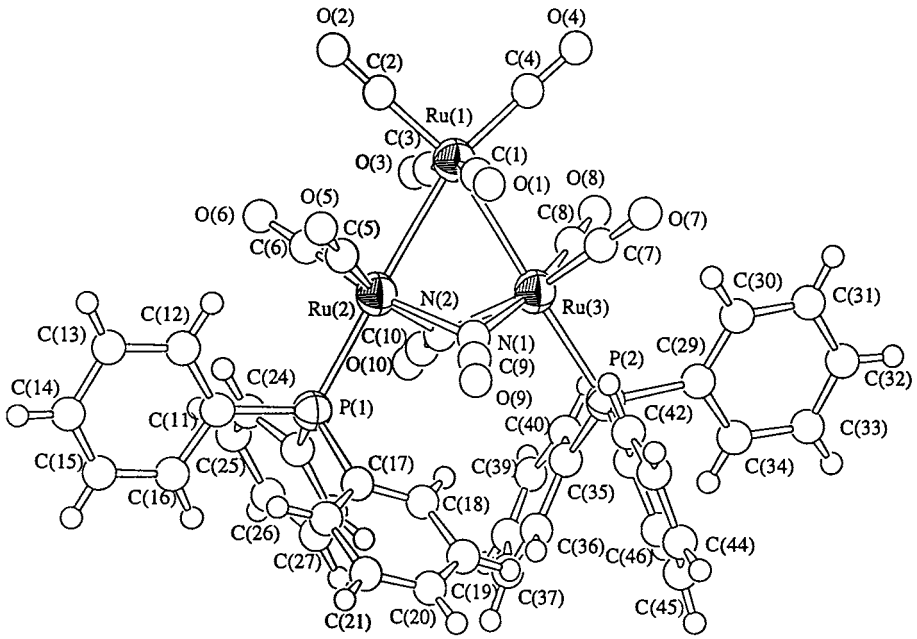

Fig. 4. The molecular structure of $[Ru_3(CO)_8(\mu\text{-NCO})(PPh_3)_2]$ **5** with the atom numbering scheme.

layer chromatographic (TLC) plates were prepared from silica (Merck Kieselgel 60 GF_{254}). Infrared spectra were recorded on a Bio-rad FTS-165 FT-IR spectrometer using 0.5 mm CaF_2 solution cells. ^{1}H-NMR spectra were obtained on a Bruker DPX-300 NMR spectrometer using deuteriated solvents as lock and reference. Fast-atom bombardment (FAB) mass spectra were recorded on a Finnigan MAT 95 mass spectrometer. Elemental analyses were performed by the Butterworth Laboratories, UK.

4.2. Reaction of $[Ru_3(CO)_9(\mu_3\text{-}CO)(\mu_3\text{-}NOMe)]$ **1** with triphenylphosphine

The solid of **1** (126 mg, 0.2 mmol) and triphenylphosphine (53 mg, 0.2 mmol) were dissolved in 50 cm^3 THF. The yellow solution was allowed to stir at room temperature for 3 days. The orange solution was then dried in vacuo and the residue was separated by preparative TLC using *n*-hexane/CH_2Cl_2 (2:1, v/v) as the eluent. Three distinct bands were observed together with a number of minor bands of yellow colour. The first yellow band with $R_f \approx 0.7$ was identified as the unreacted **1** (25 mg, 20%) from IR spectroscopy. Two yellow bands were followed and characterised as $[Ru_3(CO)_8(\mu_3\text{-}CO)(\mu_3\text{-}NOMe)(PPh_3)]$ **2** (50mg, 29%, $R_f \sim 0.5$) and $[Ru_3(CO)_7(\mu_3\text{-}CO)(\mu_3\text{-}NOMe)(PPh_3)_2]$ **3** (15mg, 7%, $R_f \approx 0.3$). The yield of cluster **2** can be increased by up to 65% when the reaction is carried out with the slow addition of a CH_2Cl_2 solution of one equivalent of Me_3NO. Similarly, cluster **3** can be obtained also in relatively higher yields (> 40%) accompanied with **2** (25%) when two equivalents of both PPh_3 and Me_3NO were used instead.

Table 5
Selected bond lengths (Å) and angles (°) of cluster **5** with estimated S.D. in parentheses

Bond lengths (Å)			
Ru(1)–Ru(2)	2.826(1)	Ru(1)–Ru(3)	2.836(1)
Ru(1)···Ru(3)	3.078(1)	Ru(2)–N(1)	2.193(9)
Ru(3)–N(1)	2.173(10)	Ru(2)–N(2)	2.182(10)
Ru(3)–N(2)	2.173(10)	Ru(2)–P(1)	2.405(4)
Ru(3)–P(2)	2.410(4)	N(1)–C(9)	1.14(2)
C(9)–O(9)	1.21(2)	N(2)–C(10)	1.17(1)
C(10)–O(10)	1.20(1)		
Bond angles (°)			
Ru(2)–Ru(1)–Ru(3)	65.87(3)	Ru(2)–N(1)–Ru(3)	89.7(3)
Ru(2)–N(2)–Ru(3)	90.0(3)	N(1)–C(9)–O(9)	178(1)
N(2)–C(10)–O(10)	175(1)		

4.3. Reaction of $[Ru_3(CO)_9(\mu_3\text{-}CO)(\mu_3\text{-}NOMe)]$ **1** with dppm

Solid of **1** (188 mg, 0.3 mmol) and dppm (115 mg, 0.3 mmol) were dissolved in 60 cm^3 THF to give a yellow solution. After stirring for 3 days, the solvent was removed from the resultant orange solution in vacuo. The residue was subjected to preparative TLC using *n*-hexane/CH_2Cl_2 (2:3, v/v) as the eluent. Three distinct yellow bands were observed in order of elution as unreacted **1** (30 mg, 16%, $R_f \approx 0.9$), $[Ru_3(CO)_{10}(\mu\text{-dppm})]$ (15 mg, 5%, $R_f \approx 0.7$) and $[Ru_3(CO)_7(\mu_3\text{-}CO)(\mu_3\text{-}NOMe)(\mu\text{-dppm})]$ **4** (100 mg, 35%, $R_f \approx 0.4$) together with a few uncharacterised yellow minor bands.

Table 6
Summary of crystallographic parameters for clusters **2**–**5**

	2	**3**	**4**	**5**
Formula	$C_{28}H_{18}NO_{10}PRu_3$	$C_{45}H_{33}NO_9P_2Ru_3{\cdot}0.5C_6H_{14}$	$C_{34}H_{25}NO_9P_2Ru_3{\cdot}0.5CH_2Cl_2$	$C_{46}H_{30}N_2O_{10}P_2Ru_3{\cdot}2CH_2Cl_2$
F_w	862.63	1140.00	999.20	1305.77
Crystal system	Monoclinic	Triclinic	Monoclinic	Orthorhombic
Space group	$P2_1/c$ (No. 14)	$P\bar{1}$ (No. 2)	$P2_1/c$ (No. 14)	$P2_12_12_1$ (No. 19)
a (Å)	15.448(2)	10.778(3)	13.234(1)	12.180(1)
b (Å)	11.837(1)	22.519(7)	15.418(1)	16.295(1)
c (Å)	16.800(2)	10.216(3)	19.269(2)	25.783(2)
α (°)	90.0	96.38(2)	90.0	90.0
β (°)	94.890(8)	105.42(2)	109.54(2)	90.0
γ (°)	90.0	82.06(2)	90.0	90.0
V (Å^3)	3060.7(5)	2360(1)	3705.2(7)	5117.2(6)
Z	4	2	4	4
$D_{calc.}$ (g cm^{-3})	1.872	1.604	1.791	1.695
$F(000)$	1680.00	1138.00	1964.00	2584.00
μ(Mo–K$_\alpha$)	15.70	10.70	14.19	12.03
Diffractometer	Rigaku–AFC7R	Rigaku-AFC7R	MAR RESEARCH image plate scanner	MAR RESEARCH image plate scanner
2θ range (°)	25	25		
Scan type	ω–2θ	ω–2θ		
Scan speed, ω (deg min^{-1})	16.0	16.0		
scan width (°)	$0.89+0.35\tan\theta$	$0.73+0.35\tan\theta$		
No. of reflections measured	4426	6560	23315	24802
No. of unique reflections	4243	6163	6973	4702
No. of reflections with $I>3\sigma(I)$	2868	3195	2747	3294
No. of variables	193	553	226	322
R[a]	0.039	0.045	0.043	0.050
R_w [b]	0.041	0.057	0.060	0.052
Largest Δ/σ	0.03	0.10	0.03	0.09
Residual electron density (e^{-3})	0.85 to −0.61	0.54 to −0.45	1.15 to −0.91	0.68 to −0.64

[a] $R = \Sigma\,||F_o|-|F_c||/\Sigma\,|F_o|$.
[b] $R_w = [\Sigma\, w(|F_o|-|F_c|)^2/\Sigma\, w(F_o)^2]^{1/2}$ where $w = [\sigma^2(F_o)]^{-1}$.

4.4. Vacuum pyrolysis of $[Ru_3(CO)_8(\mu_3\text{-}CO)(\mu_3NOMe)(PPh_3)]$ **2**

A solid sample of **2** (50 mg, 0.058 mmol) was dissolved in 5 cm^3 of CH_2Cl_2. The yellow solution was then introduced into a flame-dried Carius tube. The solvent was removed under reduced pressure to give a thin layer of **2** deposited on the inner wall of the pyrolysis tube. The tube was placed in an oven at 140°C for 1 h. The dark residue was extracted exhaustively with CH_2Cl_2. The combined extract was then concentrated to a few cm^3 and purified by preparative TLC using *n*-hexane/CH_2Cl_2 (3:2, v/v) as the eluent to give a series of minor bands with colours ranging from yellow to red. Characterisation of two major bands revealed the presence of some unreacted **2** (3 mg, 6%, $R_f \approx 0.7$) and $[Ru_3(CO)_8(\mu\text{-}NCO)_2(PPh_3)_2]$ **5** (yellow, $R_f \approx 0.5$) which was isolated as a yellow solid in 20% yield.

4.5. X-ray crystal structure determination

Single crystals of **2-5** for X-ray analyses were obtained as described above. Crystals of clusters **2** and **3** were mounted separately on top of a glass fibre by means of epoxy resin while clusters **4** and **5** were sealed in Lindemann glass capillaries. Crystal intensity data were collected on either a Rigaku-AFC7R or a MAR research image-plate scanner using graphite-monochromated Mo–K_α radiation ($\lambda = 0.71073$ Å) for unit-cell determination and data collection. Summary of the crystallographic data, structure solution and refinement are given in Table 6. The ω–2θ scan mode with speed 16.0 deg. min^{-1} was used for complexes **2** and **3**. For clusters **4** and **5**, 65 3° frames with an exposure time of 5 min per frame were used. Lorentz-polarisation and Ψ-scan absorption corrections [11] were applied to all the intensity data collected on a Rigaku-AFC7R diffractometer. However, only Lorentz and polarisation effects were corrected for **4** and **5**. An approximation to absorption correction by inter-image scaling was made. Scattering factors were taken from Ref. [12a] and anomalous dispersion effects were included in F_c [12b]. The positions of ruthenium atoms were determined by direct methods (SIR92) [13]. The remaining non-hydrogen atoms were determined by subsequent Fourier and difference Fourier syntheses. The structures were refined by full-matrix least-squares analysis on **F** with all non-hydrogen atoms refined anisotropically until convergence was reached. Hydrogen atoms of the organic moieties were generated in their ideal positions (C–H, 0.95 Å). They are included in the structure factors calculations but were not refined. All calculations were performed on a Silicon-Graphics computer using the program package TEXSAN [14].

Atomic co-ordinates, thermal parameters, and bond lengths and angles have been deposited at the Cambridge Crystallographic Data Centre (CCDC).

Acknowledgements

W.-T. Wong acknowledges financial support from the Hong Kong Research Grants Council and the University of Hong Kong. K. Ka-Hong Lee acknowledges the receipt of a postgraduate studentship, administered by the University of Hong Kong.

References

[1] K.K.H. Lee, W.T. Wong, J. Organomet. Chem. 503 (1995) 43.
[2] K.K.H. Lee, W.T. Wong, J. Chem. Soc., Dalton Trans. (1996) 1707.
[3] K.K.H. Lee, W.T. Wong, Inorg. Chem. 35 (1996) 5393.
[4] M.L. Blohm, W.L. Gladfelter, Organometallics 5 (1986) 1049.
[5] H. Shen, R.A. Senter, S.G. Bott, M.G. Richmond, Inorg. Chim. Acta. 247 (1996) 161.
[6] R.E. Stevens, R.D. Guettler, W.L. Gladfelter, Inorg. Chem. 29 (1990) 451.
[7] J.A. Smieja, W.L. Gladfelter, Inorg. Chem. 25 (1986) 2667.
[8] (a) M. Pizzotti, F. Porta, S. Cenini, F. Demartin, J. Organomet. Chem. 356 (1988), 105. (b) M. Pizzotti, S. Cenini, C. Crotti, F. Demartin, J. Organomet. Chem. 375 (1989) 123.
[9] M.I. Bruce, M.G. Humphrey, O.B. Shawkataly, M.R. Snow, E.R.T. Tiekink, J. Organomet. Chem. 315 (1986) C51.
[10] D.E. Fjare, J.A. Jensen, W.L. Gladfelter, Inorg. Chem. 22 (1983) 1774.
[11] A.C.T. North, D.C. Phillips, F.S. Mathews, Acta Crystallogr. Sect. A. 24 (1968) 351.
[12] D.T. Cromer, J.T. Waber, International Tables for X-Ray Crystallography, Kynoch Press, Birmingham, vol. 4, 1974. (a) Table 2.2.B; (b) Table 2.3.1.
[13] M.C. Burla, M. Camalli, G. Cascarano, C. Giacovazzo, G. Polidori, R. Spagna, D. Viterbo, J. Appl. Crystallogr. 22 (1989) 389.
[14] TEXSAN: Crystal Structure Analysis Package, Molecular Structure Corporation, Houston, TX, 1985 and 1992.